Hindawi Publishing Corporation
Journal of Nanomaterials
Volume 2015, Article ID 140596, 7 pages
http://dx.doi.org/10.1155/2015/140596

*Research Article*

# Fabrication of PANI/C-$TiO_2$ Composite Nanotube Arrays Electrode for Supercapacitor

**Chengcheng Zhang,[1] Changjian Peng,[1] Biao Gao,[1] Xiang Peng,[2] Xuming Zhang,[2] Jingyuan Tao,[1] Jinhan Kong,[1] and Jijiang Fu[1]**

[1]*The State Key Laboratory of Refractories and Metallurgy, School of Materials and Metallurgy, Wuhan University of Science and Technology, Wuhan 430081, China*
[2]*Department of Physics and Materials Science, City University of Hong Kong, Kowloon, Hong Kong*

Correspondence should be addressed to Biao Gao; gaobiao@wust.edu.cn and Jijiang Fu; fujijiang@wust.edu.cn

Received 18 January 2015; Accepted 17 May 2015

Academic Editor: Ovidiu Ersen



Polyaniline/carbon doped $TiO_2$ composite nanotube arrays (PANI/C-$TiO_2$ NTAs) have been prepared successfully by electrodepositing PANI in C-$TiO_2$ NTAs which were prepared by directly annealing the as-anodized $TiO_2$ NTAs under Ar atmosphere. The organic residual in the $TiO_2$ NTAs during the process of anodization acts as carbon source and is carbonized in Ar atmosphere to manufacture the C-$TiO_2$ NTAs. The specific capacitance of the PANI/C-$TiO_2$ electrode is 120.8 mF $cm^{-2}$ at a current density of 0.1 mA $cm^{-2}$ and remains 104.3 mF $cm^{-2}$ at a current density of 2 mA $cm^{-2}$ with the calculated rate performance of 86.3%. After 5000 times of charge-discharge cycling at a current density of 0.2 mA $cm^{-2}$, the specific capacitance retains 88.7% compared to the first cycle. All these outstanding performances of the as-prepared PANI/C-$TiO_2$ NTAs indicate it will be a promising electrode for supercapacitor.

## 1. Introduction

Energy shortage crisis and environmental pollution are global problems which promote the scientific research to develop clean energy and corresponding energy storage system [1, 2]. Electrochemical capacitor, also called ultracapacitor, is considered as one of the most promising energy storage devices, which is widely used to satisfy the energy demand in mobile equipments, hybrid electric vehicles, and aerospace fields because of its high power density, energy density, and excellent cycle performance [3–5]. Recently, the faradic pseudocapacitors-type supercapacitors (SCs) have attracted much attention derived from the exhibited higher specific capacitance stemming from the reversible redox reactions compared with the electric double-layer capacitors. Various pseudocapacitive materials, such as conducting polymers and transition-metal oxides/hydroxides, have been studied extensively. Among them, polyaniline (PANI) is a promising capacitive material because of its large theoretical faradic pseudocapacitance (as high as 1145 F $g^{-1}$), high conductivity, low cost, facile synthesis, and fast doping/dedoping rate [6–9]. However, the relatively poor cycle stability of PANI due to the swelling and consequent breakage of the structures during the charge-discharge process hinders its wide application [10]. Thus, maintaining the structure stability in cycling is crucial for high performance PANI-based supercapacitor [11]. PANI supported by other mechanically stable materials such as carbon nanotube, carbon nanofiber [12], graphene [13], Si [14] exhibited improved cycle stability. However, most of these supporting materials are of powder which need further mixing with conductive agent and binder before the supercapacitor assembling process, which will decrease the specific capacitance in some sense.

$TiO_2$ nanotube arrays (NTAs) fabricated directly and adhered strongly to the underlying Ti substrate by simple anodization is a promising supporting material for PANI loading, which provides large active surface areas and robust scaffold. Its hydrophilic surface and controllable dimension (including diameter and tube spacing) in favor of the uniform deposition and efficient utilization of conducting polymer

[15, 16]. However, $TiO_2$ with poor conductivity hinders electrodepositing PANI and goes against the rate ability of supercapacitor. In very recently, we improved the conductivity of $TiO_2$ by directly nitriding $TiO_2$ NTAs to form well conductive TiN NTAs acting as support materials for loading PANI and MoOx, which exhibits high specific capacitance and excellent cycle stability [17, 18].

In this work, we demonstrated another conductive support material, carbon doped $TiO_2$ nanotube arrays (C-$TiO_2$ NTAs), to maintain the PANI structure. PANI can be easily deposited on the surface to form uniform PANI and C-$TiO_2$ nanotube arrays (PANI/C-$TiO_2$ NTAs) by the electrochemical deposition. Because of directional channel for electrons transport and the suitable tube space for the electrolyte permeating, the PANI/C-$TiO_2$ NTAs electrode exhibits high specific capacitance of 120.8 mF $cm^{-2}$ at the current density of 0.1 mA $cm^{-2}$ and it also remains 86.3% when the current density increases to 2 mA $cm^{-2}$. It expresses wonderful cycling performance with the specific capacitance retention of 88.7% even after 5000 cycles. The results demonstrate that the synthesized PANI/C-$TiO_2$ NTAs nanocomposite has great potential applications for SCs.

## 2. Experimental Details

All chemicals used are of analytical grade. Electrochemical anodization was adopted for $TiO_2$ preparation with a typical two-electrode configuration of electrochemical anodization where a piece of Ti foil (1·1·0.5 $cm^3$) was used as anode and a piece of graphite plate was served as cathode with 1 cm separation, powered by a direct current power supply (IT6834, ITECH, China). The electrolyte was $NH_4F$ (0.5 wt.%), $CH_3OH$ (5 vol.%), and deionized water (5 vol.%) in ethylene glycol. The applied potential was 60 V and lasted for 30 min.

To produce the C-$TiO_2$ NTAs, we developed an easy annealing processing by utilizing the residual organic agency after anodization in ethylene glycol based electrolyte. In detail, the as-anodized $TiO_2$ NTAs was directly calcined in a tube furnace at 500°C for 3 h in Ar atmosphere with the heating rate of 15°C/min [19, 20].

Controlled electropolymerization was used in a three-electrode system with a Pt foil (2·2 $cm^2$) as the counter electrode, saturated calomel electrode (SCE) as the reference electrode, $TiO_2$ NTAs and C-$TiO_2$ NTAs as the working electrode to fabricate the composite NTAs. In general, the C-$TiO_2$ NTAs was used as working electrode which was subjected to repeating potential scanning in 0.5 M $H_2SO_4$ solution containing 0.05 M aniline in the range from −0.6 to 1.0 V at the scan rate of 50 mV/s for 15 and 30 cycles, respectively.

The samples were characterized by SEM (FE-SEM, FEI Nova 400 Nano), X-ray diffraction (XRD, Philips X′ Pert Pro) with Cu K$\alpha$ radiation of wavelength of 1.5416 Å in the range of 20–80° (2$\theta$), FTIR Spectrometer (Perkin Elmer 1600), and X-ray photoelectron spectroscopy (ESCALB MK-II, VG Instruments, U.K.).

Electrochemical measurements were carried out using a CHI 660C instrument. The three-electrode cell consisted of a SCE as the reference electrode, a 2·2 $cm^2$ platinum plate as the counter electrode, and PANI/C-$TiO_2$ sample (1·1 $cm^2$) as the working electrode. 1 M $H_2SO_4$ solution served as the electrolyte at room temperature. The cyclic voltammetry (CV) was performed between 0 and 1 V (versus SCE) at different scanning rate. Galvanostatic charge-discharge curves were measured at different current density over the voltage range of 0–0.6 V (versus SCE). Cycling stability performance was conducted with a charge-discharge tester (Land CT2001A, Wuhan LAND Electronics Co., Ltd., China).

## 3. Results and Discussion

Figures 1(a) and 1(b) show the SEM images of $TiO_2$ NTAs and C-$TiO_2$ NTAs obtained from annealing as-anodized $TiO_2$ NTAs under air and Ar, respectively. It is obvious that the morphologies of $TiO_2$ NTAs and C-$TiO_2$ NTAs are of no significant difference. The as-obtained highly ordered and well-separated C-$TiO_2$ NTAs have a length of about 9 $\mu$m, interior diameter of about 110 nm, and tube wall thickness of about 20–25 nm. As the XRD pattern of $TiO_2$ NTAs and C-$TiO_2$ NTAs shown in Figure 1(c), the diffraction peaks can be attributed to anatase $TiO_2$ and titanium substrate; and no distinguished difference is observed between the $TiO_2$ NTAs (1) and C-$TiO_2$ NTAs (2). Figure 1(d) displays the XPS full spectra for $TiO_2$ NTAs (1) and C-$TiO_2$ NTAs (2). C, Ti, and O peaks are observed for C-$TiO_2$ NTAs, while only Ti and O peaks are observed for $TiO_2$ NTAs. The top right corner inset shows the high-resolution C 1s spectra. The peak at 281.9 and weak peak at 284.6 eV are attributed to Ti-C and C-C [21]. The XPS results indicate that carbon was doped into the $TiO_2$ NTAs through the residual ethylene glycol reacting with the as-anodized amorphous $TiO_2$ during annealing in Ar. While during heating in air, the residual ethylene glycol can react with $O_2$ forming $CO_2$ and $H_2O$ resulting in formatting pure $TiO_2$ NTAs. Figures 1(e) and 1(f) show the electrochemical impedance spectroscopy of $TiO_2$ NTAs and C-$TiO_2$ NTAs, respectively, to identify their conductivity. Compared to the resistance of the $TiO_2$ NTAs (20 kΩ), the resistance of C-$TiO_2$ NTAs decreased by 3 orders of magnitude to 18 Ω. It indicates that the C-$TiO_2$ NTAs has an excellent conductivity, which will be of benefit for aniline monomer electropolymerizing on tube wall.

Figures 2(a) and 2(b) show the SEM images of the PANI deposited on $TiO_2$ NTAs and C-$TiO_2$ NTAs by electropolymerization in 0.05 M aniline sulfuric acid solution for 15 cycles, named PANI/$TiO_2$-15 and PANI/C-$TiO_2$-15, respectively. The typical PANI/C-$TiO_2$-15 nanotube has a smaller interior diameter of 80 nm and its tube wall is 35–40 nm which is thicker than that of the C-$TiO_2$ NTAs due to the PANI depositing. However, for the PANI/$TiO_2$-15, the diameter and tube wall are the same as the origin $TiO_2$ nanotube. The inset is corresponding electrochemical CV curves of the PANI deposition process of them. As for C-$TiO_2$ NTAs, obvious redox peaks were observed and the peak current increases with the cycle number increasing which

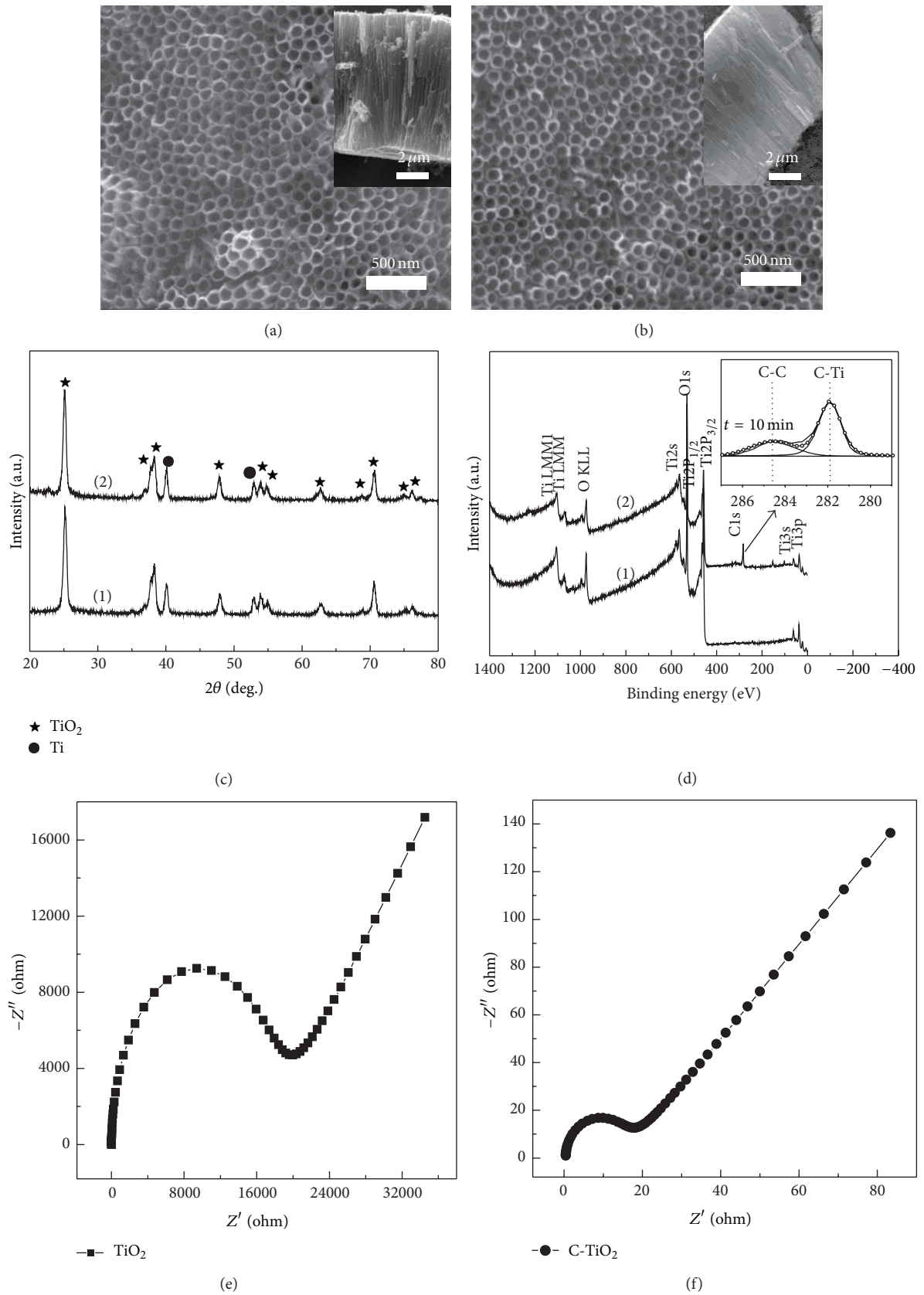


FIGURE 1: SEM images of top- and cross-section (inset) of $TiO_2$ NTAs (a) and C-$TiO_2$ NTAs (b), XRD patterns (c) and XPS full spectra (d) of $TiO_2$ NTAs (1) and C-$TiO_2$ NTAs for (2), the inset of (d) is the fine spectra of C 1s; EIS plots of $TiO_2$ NTAs (e) and C-$TiO_2$ NTAs (f) in 1 M $H_2SO_4$ solution.

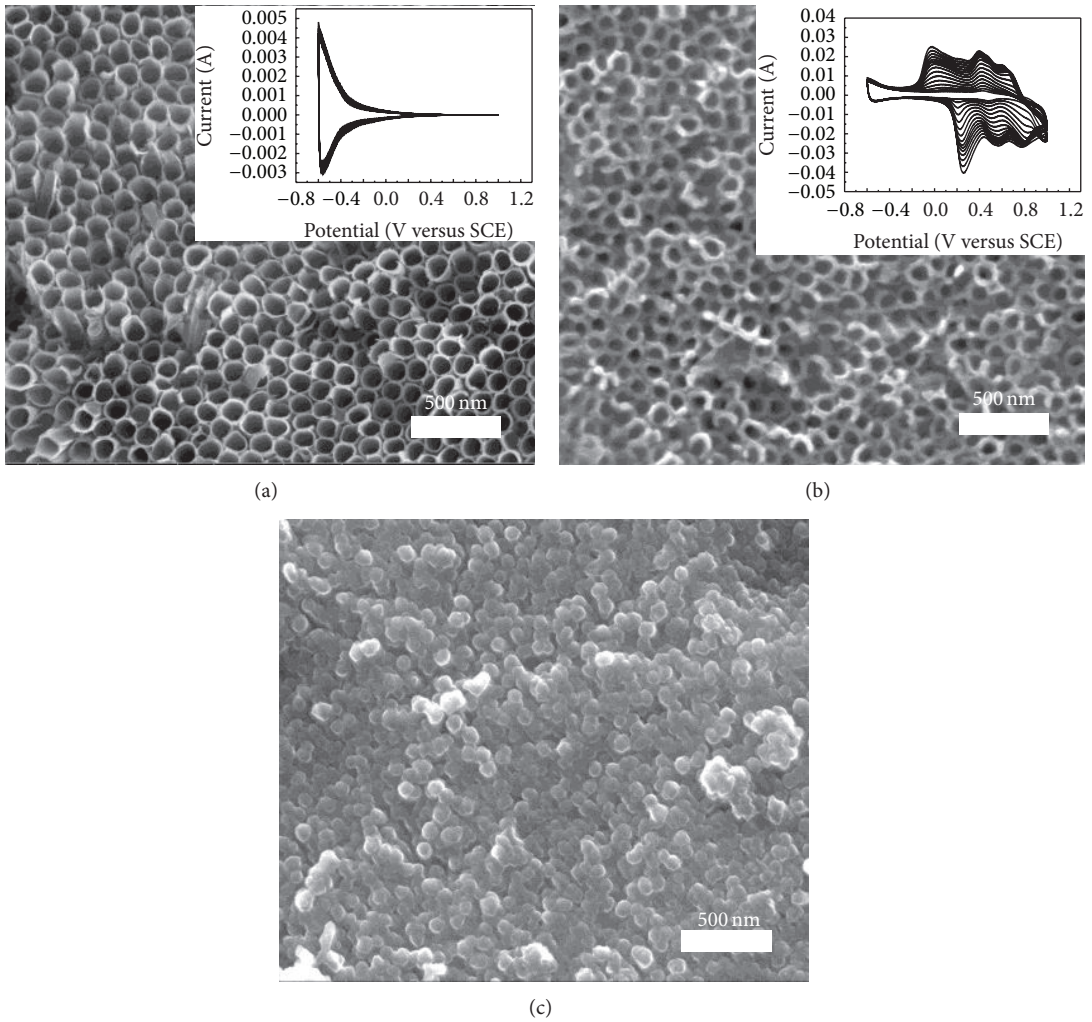


Figure 2: SEM for $TiO_2$ (a) and C-$TiO_2$ (b) deposited in 0.05 M aniline sulfuric acid solution for 15 cycles; inset picture is their corresponding CV plots of polymerization process; (c) is PANI/C-$TiO_2$ for 30 cycles.

indicates that polymerization reaction has occurred. However, redox peak was not appeared at the CV curves collected for $TiO_2$ NTAs during whole deposition. These results suggest that C-$TiO_2$ NTAs are easier for electrochemical deposition for PANI due to the enhanced conductivity compared to $TiO_2$ NTAs. The SEM image of PANI/C-$TiO_2$-30 is shown in Figure 2(c) indicating that the C-$TiO_2$ nanotubes are packed by the deposited PANI after polymerizing for 30 cycles. It would block the electrolyte from contacting the inner PANI resulting in the fact that it will not be possible to make full use of the as-polymerized PANI. On the other hand, the accumulated PANI because of lacking firmly support may be easy to topple down which is antagonistic to the cycle stability and rate capability.

The FTIR spectrum of the C-$TiO_2$ NTAs before and after depositing PANI is shown in Figure 3. For C-$TiO_2$ in curve (1), the peak at 1350 $cm^{-1}$ is attributed to the formation of carbonate or carboxylate species and the peak at 1600 $cm^{-1}$ corresponding to the stretching vibration modes of water or hydroxyl groups absorbed on C-$TiO_2$ [22]. Besides, the two peaks at 1349 $cm^{-1}$ and 1599 $cm^{-1}$ are attributed to the formation of carbonate or carboxylate species and hydroxyl groups, respectively; other peaks are found for PANI/C-$TiO_2$ (curve (2)). The peaks at 1561 and 1483 $cm^{-1}$ belonged to the C=C stretching of the quinoid ring and benzenoid ring, respectively. Those at 1263 and 1168 $cm^{-1}$ are attributed to C-N stretching of the secondary aromatic amine. The peak at 813 $cm^{-1}$ is ascribed to the out-of-plane bending of C-H on the 1,4-disubstituted ring. The peak at 1220 $cm^{-1}$ can be attributed to various stretching and bending vibrations associated with the C-C bond [23]. The peak at 1168 $cm^{-1}$ is referred to as the "electronic-like band," and its intensity is considered as a measure of the degree of delocalization of electrons on polyaniline [24]. From the FTIR spectra, it can be further concluded that PANI was deposited onto the C-$TiO_2$ NTAs nanocomposite electrode after the electrochemical deposition process.

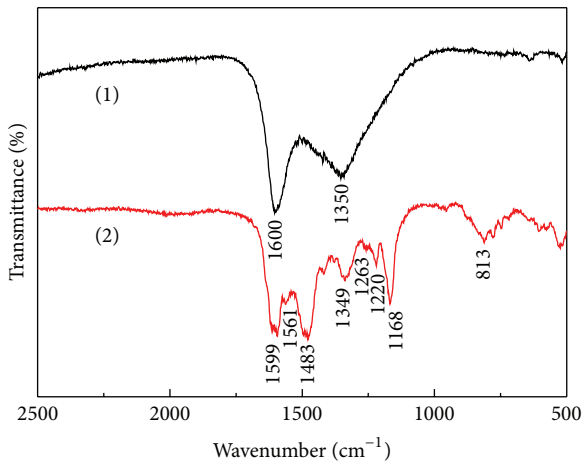


FIGURE 3: FTIR spectrum of C-$TiO_2$ and PANI/C-$TiO_2$.

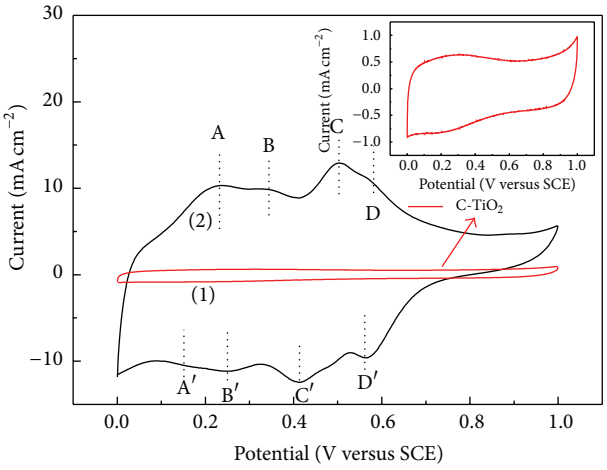


(1) C-$TiO_2$
(2) PANI/C-$TiO_2$-15

FIGURE 4: CV curves of C-$TiO_2$ and PANI/C-$TiO_2$-15 at a scan rate of 50 mV s$^{-1}$.

CV tests were performed to study the electrochemical properties of the PANI/C-$TiO_2$ NTAs electrode in 1 M $H_2SO_4$ solution. As shown in Figure 4, CV curve of PANI/C-$TiO_2$-15 NTAs displays a larger area compared with that of the original C-$TiO_2$ NTAs at the scan rate of 50 mV s$^{-1}$. It exhibits four pairs of redox peaks of PANI, which implies a high pseudocapacitance. The first pair of redox peaks A/A′ (at 0.23/0.15 V) can be ascribed to the transformation between emeraldine and pernigraniline states [15]; the peaks B/B′ (at 0.34/0.25 V) and C/C′ (at 0.50/0.41 V) derived mainly from the redox reactions of dimers, oligomers, and the degradation products including p-benzoquinone, quinoneimine, p-aminodiphenylamine, hydroquinone, and p-aminophenol [23, 25] and the peaks D/D′ (at 0.58/0.56 V) can be ascribed to the transformation between emeraldine and pernigraniline states [17].

Figure 5(a) shows the charge/discharge curves of PANI/C-$TiO_2$-15 NTAs electrode at the current density of 0.1, 0.2, 0.5, 1, and 2 mA cm$^{-2}$. As a comparison, the charge/discharge curves of C-$TiO_2$, PANI/C-$TiO_2$-15 and PANI/C-$TiO_2$-30 at 0.1 mA cm$^{-2}$ are shown in Figure 5(b). Their specific capacitances are calculated according to the formula as follows:

$$C_A = \frac{C}{A} = \frac{I \times \Delta t}{\Delta V \times A}, \quad (1)$$

where $C_A$ is the specific capacitance, $I$ is the charge/discharge current density, $\Delta t$ is the discharge time, $\Delta V$ is the potential range, and $A$ denotes apparent area of the electrode. The specific capacitance of PANI/C-$TiO_2$-15 NTAs is calculated to be 120.8, 119.3, 116.1, 111.7, and 104.3 mF cm$^{-2}$ at a current density of 0.1, 0.2, 0.5, 1, and 2 mA cm$^{-2}$ shown in Figure 5(c). In contrast, the specific capacitance of C-$TiO_2$ and PANI/C-$TiO_2$-30 NTAs is calculated to be 16.1, 14.5, 13.5, 12.5, and 12.3 mF cm$^{-2}$ and 202.4, 163.8, 109.8, 89.9, and 79.7 mF cm$^{-2}$ at the corresponding current density, respectively. It can be seen that both PANI/C-$TiO_2$-15 and PANI/C-$TiO_2$-30 NTAs show enhanced performance after the electropolymerization. It is worth mentioning that the specific capacitance of PANI/C-$TiO_2$-30 NTAs is higher than that of the PANI/C-$TiO_2$-15 NTAs at a lower current density because of the large amount of the loading mass of PANI per cm$^2$. However, when the current density increases to 0.5 mA cm$^{-2}$, the areal capacitance becomes smaller than the PANI/C-$TiO_2$-15 NTAs due to the poor ion diffusion in blocked nanotube of the PANI/C-$TiO_2$-30.

Cycling performance is also one of the most important properties of supercapacitor. Cycling test of PANI/C-$TiO_2$-15 NTAs electrode was carried out at a current density of 0.2 mA cm$^{-2}$ in 1 M $H_2SO_4$ solution in the potential range of 0–0.6 V (versus SCE). Figure 5(d) shows the curve of capacitance changes with the cycle number increasing. After 5000 cycles, the capacitance retention is as high as 88.7%. This excellent cycle stability of PANI/C-$TiO_2$-15 NTAs electrode resulted from the structure stability of C-$TiO_2$ NTAs during charge-discharge process.

## 4. Conclusions

In summary, the PANI/C-$TiO_2$ NTAs electrode was prepared by depositing PANI on the conductive C-$TiO_2$ NTAs obtained from directly annealing the as-anodized $TiO_2$ NTAs under Ar atmosphere. The PANI/C-$TiO_2$-15 NTAs electrode performs a good specific capacitance of 120.8 mF cm$^{-2}$ and good rate ability with capacitance retention of 86.3% when the current density increases 20 times. Due to the structure stability of C-$TiO_2$ NTAs, PANI/C-$TiO_2$ nanocomposite electrode expresses wonderful cycling performance that the specific capacitance remains 88.7% even after 5000 cycles. All these outstanding performances make this composite material a promising electrode in the field of energy storage.

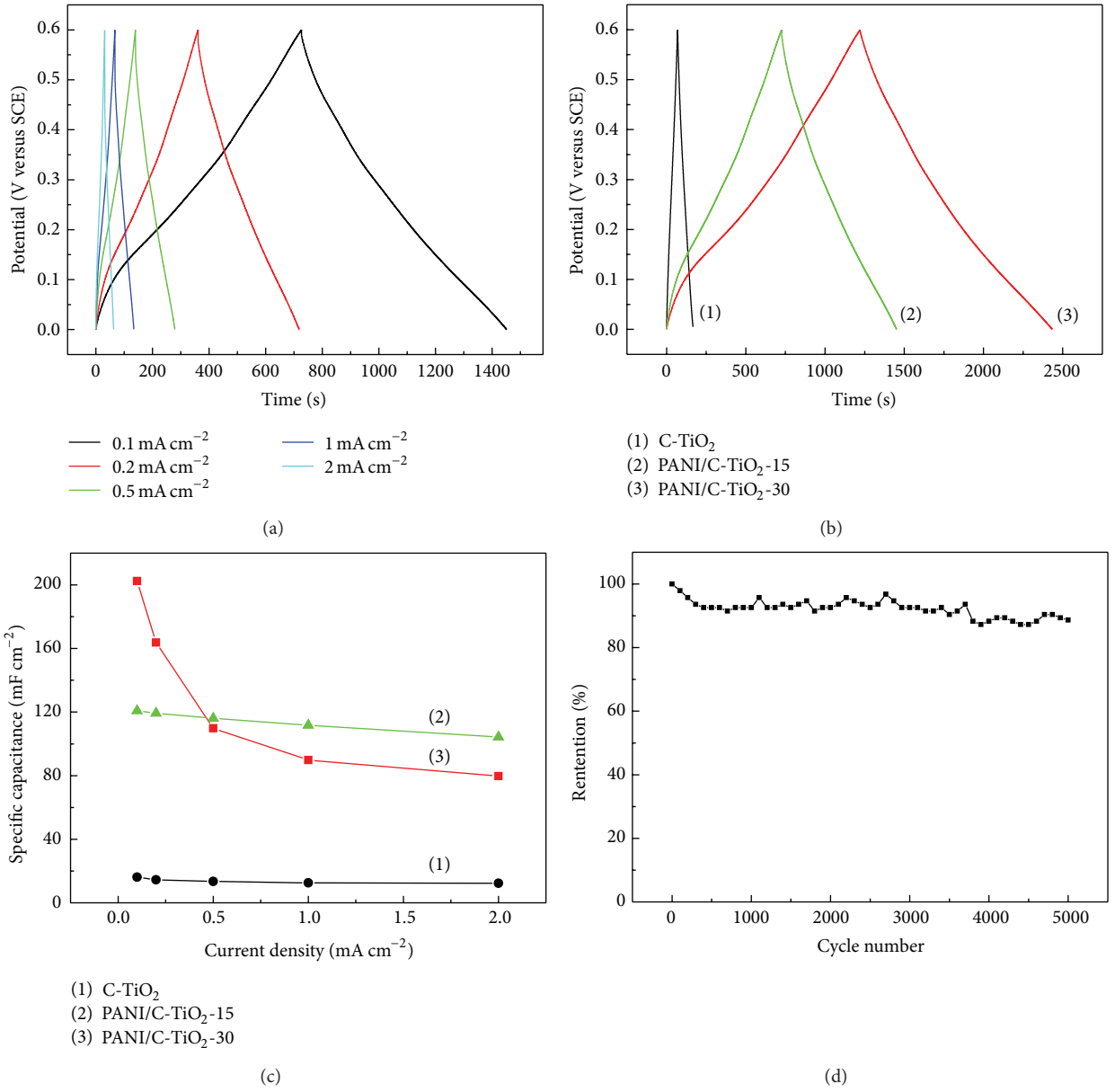


Figure 5: (a) Charge/discharge curves of PANI/C-$TiO_2$-15 at different current densities of 0.1, 0.2, 0.5, 1, and 2 mA cm$^{-2}$. (b) Charge/discharge curves of C-$TiO_2$, PANI/C-$TiO_2$-15, and PANI/C-$TiO_2$-30 at 0.1 mA cm$^{-2}$. (c) Rate performance of C-$TiO_2$, PANI/C-$TiO_2$-15, and PANI/C-$TiO_2$-30. (d) Cycling performance of the PANI/C-$TiO_2$-15 electrode at a current density of 0.2 mA cm$^{-2}$ in 1 M $H_2SO_4$.

## Conflict of Interests

The authors declare that there is no conflict of interests regarding the publication of this paper.

## Authors' Contribution

Chengcheng Zhang and Changjian Peng contributed equally to this work.

## Acknowledgments

This work was financially supported by Young Scientific and Technological Backbone Cultivating Project of Wuhan University of Science and Technology (no. 2013xz002), the Outstanding Young and Middle-Aged Scientific Innovation Team of Colleges and Universities of Hubei Province (T201402), the Natural Science Foundation of Hubei Province (2013CFB327), and the Applied Basic Research Program of Wuhan City (2013011801010598).

## References

[1] C. Liu, F. Li, L. P. Ma, and H. M. Cheng, "Advanced materials for energy storage," *Advanced Materials*, vol. 22, no. 8, pp. E28–E62, 2010.

[2] H. Wang, H. Feng, and J. Li, "Graphene and graphene-like layered transition metal dichalcogenides in energy conversion and storage," *Small*, vol. 10, no. 11, pp. 2165–2181, 2014.

[3] J. Yan, Q. Wang, T. Wei, and Z. Fan, "Recent advances in design and fabrication of electrochemical supercapacitors with high energy densities," *Advanced Energy Materials*, vol. 4, no. 4, Article ID 1300816, 2014.

[4] G. Yu, X. Xie, L. Pan, Z. Bao, and Y. Cui, "Hybrid nanostructured materials for high-performance electrochemical capacitors," *Nano Energy*, vol. 2, no. 2, pp. 213–234, 2013.

[5] A. L. M. Reddy, S. R. Gowda, M. M. Shaijumon, and P. M. Ajayan, "Hybrid nanostructures for energy storage applications," *Advanced Materials*, vol. 24, no. 37, pp. 5045–5064, 2012.

[6] J. Yan, T. Wei, B. Shao et al., "Preparation of a graphene nanosheet/polyaniline composite with high specific capacitance," *Carbon*, vol. 48, no. 2, pp. 487–493, 2010.

[7] C. Peng, D. Hu, and G. Z. Chen, "Theoretical specific capacitance based on charge storage mechanisms of conducting polymers: comment on 'Vertically oriented arrays of polyaniline nanorods and their super electrochemical properties'," *Chemical Communications*, vol. 47, no. 14, pp. 4105–4107, 2011.

[8] X. Y. Zhao, J. B. Zang, Y. H. Wang, L. Y. Bian, and J. K. Yu, "Electropolymerizing polyaniline on undoped 100 nm diamond powder and its electrochemical characteristics," *Electrochemistry Communications*, vol. 11, no. 6, pp. 1297–1300, 2009.

[9] L. Xiao, Y. Cao, J. Xiao et al., "A soft approach to encapsulate sulfur: polyaniline nanotubes for lithium-sulfur batteries with long cycle life," *Advanced Materials*, vol. 24, no. 9, pp. 1176–1181, 2012.

[10] J. Yan, T. Wei, Z. Fan et al., "Preparation of graphene nanosheet/carbon nanotube/polyaniline composite as electrode material for supercapacitors," *Journal of Power Sources*, vol. 195, no. 9, pp. 3041–3045, 2010.

[11] E. Frackowiak, V. Khomenko, K. Jurewicz, K. Lota, and F. Béguin, "Supercapacitors based on conducting polymers/nanotubes composites," *Journal of Power Sources*, vol. 153, no. 2, pp. 413–418, 2006.

[12] X. Yan, Z. Tai, J. Chen, and Q. Xue, "Fabrication of carbon nanofiber-polyaniline composite flexible paper for supercapacitor," *Nanoscale*, vol. 3, no. 1, pp. 212–216, 2011.

[13] K. Zhang, L. L. Zhang, X. S. Zhao, and J. Wu, "Graphene/polyaniline nanofiber composites as supercapacitor electrodes," *Chemistry of Materials*, vol. 22, no. 4, pp. 1392–1401, 2010.

[14] W. Wang and E. A. Schiff, "Polyaniline on crystalline silicon heterojunction solar cells," *Applied Physics Letters*, vol. 91, no. 13, Article ID 133504, 2007.

[15] K. Xie, J. Li, Y. Lai et al., "Polyaniline nanowire array encapsulated in titania nanotubes as a superior electrode for supercapacitors," *Nanoscale*, vol. 3, no. 5, pp. 2202–2207, 2011.

[16] K. Siuzdak, M. Sawczak, and A. Lisowska-Oleksiak, "Fabrication and properties of electrode material composed of ordered titania nanotubes and pEDOT:PSS," *Solid State Ionics*, vol. 271, pp. 56–62, 2015.

[17] X. Peng, K. Huo, J. Fu, X. Zhang, B. Gao, and P. K. Chu, "Coaxial PANI/TiN/PANI nanotube arrays for high-performance supercapacitor electrodes," *Chemical Communications*, vol. 49, no. 86, pp. 10172–10174, 2013.

[18] X. Peng, K. Huo, J. Fu et al., "Porous dual-layered $MoO_x$ nanotube arrays with highly conductive TiN cores for supercapacitors," *ChemElectroChem*, vol. 2, no. 4, pp. 512–517, 2015.

[19] L. Hu, K. Huo, R. Chen, B. Gao, J. Fu, and P. K. Chu, "Recyclable and high-sensitivity electrochemical biosensing platform composed of carbon-doped $TiO_2$ nanotube arrays," *Analytical Chemistry*, vol. 83, no. 21, pp. 8138–8144, 2011.

[20] X. Peng, J. Fu, X. Zhang et al., "Carbon-doped $TiO_2$ nanotube array platform for visible photocatalysis," *Nanoscience and Nanotechnology Letters*, vol. 5, no. 12, pp. 1251–1257, 2013.

[21] I. C. Kang, Q. Zhang, S. Yin, T. Sato, and F. Saito, "Preparation of a visible sensitive carbon doped $TiO_2$ photo-catalyst by grinding $TiO_2$ with ethanol and heating treatment," *Applied Catalysis B: Environmental*, vol. 80, no. 1-2, pp. 81–87, 2008.

[22] L. Zhang, M. S. Tse, O. K. Tan, Y. X. Wang, and M. Han, "Facile fabrication and characterization of multi-type carbon-doped $TiO_2$ for visible light-activated photocatalytic mineralization of gaseous toluene," *Journal of Materials Chemistry A*, vol. 1, no. 14, pp. 4497–4507, 2013.

[23] J. Kan, R. Lv, and S. Zhang, "Effect of ethanol on properties of electrochemically synthesized polyaniline," *Synthetic Metals*, vol. 145, no. 1, pp. 37–42, 2004.

[24] Z. Wang, S. Liu, P. Wu, and C. Cai, "Detection of glucose based on direct electron transfer reaction of glucose oxidase immobilized on highly ordered polyaniline nanotubes," *Analytical Chemistry*, vol. 81, no. 4, pp. 1638–1645, 2009.

[25] V. Khomenko, E. Frackowiak, and F. Béguin, "Determination of the specific capacitance of conducting polymer/nanotubes composite electrodes using different cell configurations," *Electrochimica Acta*, vol. 50, no. 12, pp. 2499–2506, 2005.